



## Cusp flows due to an extended sink in two dimensions

A. J. KOERBER and L. K. FORBES

*Department of Mathematics, University of Queensland, St. Lucia, Queensland 4072, Australia*

Received 3 June 1998; accepted in revised form 11 February 1999

**Abstract.** The steady two-dimensional potential flow of a finite-depth fluid into an extended or distributed sink, in which the free surface dips to form a cusp above the centre of the sink, is examined. The extended sink is a region where the vertical outflow velocity  $V$  is constant and uniform. Numerical solutions for the free-surface profiles are obtained by use of a boundary-integral technique. Solutions are only found for the supercritical case where the Froude numbers are greater than one. In the limiting case where the extended sink width tends to zero, the problem reduces to that of a line sink beneath the free surface, and comparisons are made to existing results for this type of flow.

**Key words:** withdrawal flow, free surface, boundary integral, cusp.

### 1. Introduction

Flows associated with the withdrawal of a fluid from a reservoir of some nature have been given a fair amount of attention over the past couple of decades. Examples of such reservoirs are dams, water reservoirs and cooling ponds (Imberger and Hamblin [1]), and the interest may be motivated by a desire to control water quality. Most of the mathematical attention given to these problems has been focused on the flow caused by a line sink or source beneath the free surface. Two types of flow are known to exist for this configuration, namely stagnation-point flows, where the free surface rises to a stagnation point above the sink (see for example Mekias and Vanden-Broeck [2]), and cusp flows, where the free surface dips to form a vertically sloped cusp above the sink. That the cusp must be vertical is discussed in Tuck and Vanden-Broeck [3]. We shall be concerned only with this second type of flow.

It should be noted that mathematically there is no distinction between the flow caused by a line sink or a source, since the formulation depends only on the square of the Froude number, which is a nondimensional measure of the far-field fluid velocity, so that there is no mechanism for specifying the flow direction. Physically it would seem more likely that cusp solutions are associated with a line sink rather than a source. In an experiment performed by Imberger [4] with a line sink, stagnation point flows were found up to some critical Froude number, at which point the surface ‘jumped’ to a cusp. This is evidence that cusp flows certainly exist for a sink, but the fact that stagnation point flows exist for a sink, as well as a source, complicates the issue. Tyvand [5] considered a small-time expansion for the unsteady flow due to an impulsively started line source or sink in infinite depth, and found that there was a rise or drop in the surface height above the source or sink, respectively. This indicates that sources and sinks experience different time histories, but it is not clear that they could not both evolve to the same steady state.

In three dimensions, steady cusp flows have not been observed for axisymmetric withdrawal into a point sink. Forbes and Hocking [6] and Forbes, Hocking and Chandler [7] sought

such solutions for the infinite and finite depth cases, respectively, using the techniques they employed to find three-dimensional stagnation point solutions, but without success. However, a number of publications (Zhou and Graebel [8], Miloh and Tyvand [9], and Xue and Yue [10]) report transient free-surface dips, which are cusp-like in nature, as the free surface drops into the sink, but again no steady cusp solutions are found. It seems likely that the finite extent of any physical sink would become important once the free surface has dropped into the sink. It is therefore possible that the steady cusp-like solutions with constant circulation of Forbes and Hocking [11], which describe flow into a circular drain of finite radius, may exist as an evolutionary endpoint for the transient flows.

For two-dimensional flow in an infinite depth fluid, a cusp solution for a line source was found by Tuck and Vanden-Broeck [3] at a unique value of the Froude number. Hocking [12] found cusp solutions for a line sink or source above a flat or sloping bottom, and this work was continued by Vanden-Broeck and Keller [13]. For a sloping bottom only unique solutions are found, but for a flat bottom, solutions are found for all values of the Froude number  $F > 1$ . Vanden-Broeck and Keller [13] also found a unique branch of cusp solutions for sub-critical flow,  $F < 1$ . Hocking [14] and King and Bloor [15] found solutions in the infinite Froude number limit for a source or sink above a flat bottom.

There are at least two logical extensions of the above problem. One is to consider the withdrawal from a two-layer fluid as in Hocking [16] for example. Therein Hocking provides a quite thorough review of the literature. Subsequently, Hocking [17] describes the persistence of cusp-like solutions for supercritical flow in infinite depth, in which both the upper and lower fluid are being withdrawn by the sink. In this case, the interface enters the line sink itself, and therefore nonvertical cusp solutions can be sustained. Indeed, vertical cusp solutions represent the limit at which point the upper layer ceases to flow, and the problem reduces to one of a single layer.

Another possible extension is to consider a sink region of finite width. Hocking [18] and later Hocking and Vanden-Broeck [19] consider the flow of a finite-depth fluid into a vertical slot, which is quite similar to the subject of the present paper, although here, the withdrawal occurs through a horizontal mat on the bottom. As mentioned above in the discussion of the three-dimensional problem, it would seem likely that the finite extent of a physical sink becomes important for flows in which the free surface approaches the sink.

We consider the two-dimensional flow into an extended or distributed sink of a finite-depth fluid. The extended sink is a region along the bottom where the vertical outflow velocity is specified, and we only consider the case where it is fixed to have a uniform value  $V$  along the length of the sink. In practice such a flow could be produced in a large rectangular tank with some kind of mesh across a slot on the bottom of the tank connected to a pump to generate the uniform outflow velocity.

Since this flow is symmetric about the centre of the extended sink and we neglect viscosity, the resultant flow would be the same as if there were a vertical wall placed at the centre of the sink. The cusp point would then be where the free surface smoothly attaches to the vertical wall. We exploit this fact in the following mathematical formulation by explicitly considering the wall to be present. This is found to lead to more accurate numerical solutions than if the wall were not explicitly included, as the presence of the wall helps enforce the smooth attachment, or the vertical free surface slope at the cusp point.

We formulate the problem as a boundary-integral equation, using Cauchy's integral formula, and this is then solved numerically by a damped Newton iterative scheme.

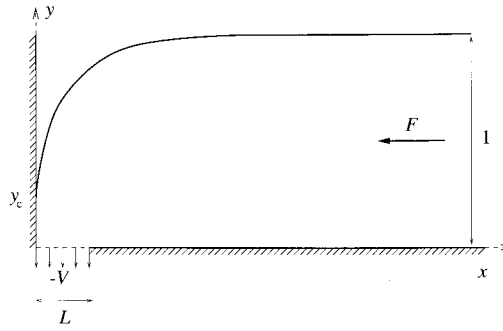


Figure 1. A sketch in dimensionless coordinates showing the flow of fluid from right to left into an extended sink in a corner.

## 2. Formulation of the problem

We model the free-surface flow from right to left of a fluid into an extended sink in a corner, as shown in Figure 1, assuming a two-dimensional geometry. The origin of the  $(x, y)$  coordinate system is chosen to coincide with the bottom left corner of the flow region. The extended sink is the region along the bottom between the origin and the point  $L$ , across which fluid is withdrawn with a constant and uniform vertical velocity  $V$ .

All lengths have been nondimensionalised with respect to the undistributed far-stream depth  $H$ , and all velocities have been nondimensionalised by the velocity scale  $\sqrt{gH}$ . The far-stream depth is therefore 1, the width of extended sink becomes  $L$  and the far-stream velocity becomes  $F = U/\sqrt{gH}$ , which is the Froude number, where  $U$  is the dimensional far-stream velocity towards the sink. The constant outflow velocity  $V$  through the extended sink is, by conservation of mass,  $V = F/L$ . Lastly, the height of the free surface above the sink, where it smoothly attaches to the vertical wall at  $x = 0$  forming a cusp, is denoted by  $y_c$ .

By assuming the flow is irrotational and the fluid is incompressible and inviscid, our task is to solve Laplace's equation in the fluid region for the velocity potential  $\phi$ , subject to the appropriate boundary conditions. If we denote the horizontal and vertical fluid velocity components by  $u$  and  $v$ , respectively, then the boundary condition along the flat bottom  $y = 0$  is,

$$v = \begin{cases} 0 & x > L \\ -V & 0 \leq x \leq L \end{cases} \quad (1)$$

and on the vertical wall  $x = 0$  we have

$$u = 0 \quad 0 \leq y \leq y_c. \quad (2)$$

Let  $y = \eta(x)$  be the location of the free surface; then the boundary conditions on  $y = \eta$  are Bernoulli's equation,

$$\frac{1}{2}(u^2 + v^2) + \eta = \frac{1}{2}F^2 + 1 \quad (3)$$

and the kinematic condition,

$$u \frac{d\eta}{dx} = v. \quad (4)$$

Instead of attempting to solve Laplace's equation directly, we shall formulate the problem as a boundary integral along the free surface. To this end, we introduce the complex variable  $z = x + iy$  and the complex potential  $f(z) = \phi + i\psi$ , where  $\psi$  is the streamfunction.

We next construct an analytic function  $\chi(z)$  such that

$$\chi(z) = \frac{df}{dz} - \frac{dg}{dz} = u - iv - (\mu - i\nu). \quad (5)$$

The function  $g(z)$  is the complex potential obtained for flow into a corner with a 'rigid lid', that being the case where the free surface  $y = \eta(x)$  has been replaced by the solid boundary  $y = 1$ . The horizontal and vertical velocity components of this rigid-lid solution are  $\mu$  and  $\nu$ , respectively. It can be shown (see Appendix) that the closed form solution for  $dg/dz$  is

$$\frac{dg}{dz} = -\frac{2V}{\pi} \operatorname{arctanh} \left( \coth \left( \frac{\pi z}{2} \right) \tanh \left( \frac{\pi L}{2} \right) \right). \quad (6)$$

Reflecting the flow about the  $x$ -axis, we observe that  $\chi(z)$  has the desirable properties of being analytic everywhere in the combined flow/image flow region, and tending to zero as  $x$  tends to infinity. Cauchy's Integral Formula is now used to give

$$\oint_{\Gamma} \frac{\chi(\xi) d\xi}{\xi - z} = 0, \quad (7)$$

where  $\xi$  is a point on the curve  $\Gamma$  and we take  $z$  to lie on  $\Gamma$  also. We define  $\Gamma$  to be the positively oriented contour made up of the free surface, the vertical wall along the  $y$ -axis from  $y = 0$  to  $y = y_c$ , the reflection of the wall about  $y = 0$ , the image free surface and a vertical line at  $x = \infty$  connecting the free surface and its image. The point  $z$  lying on the real boundary is bypassed by a semicircle of vanishingly small radius.

We parametrise the free surface by the arclength  $t$ , and denote the point  $\xi$  on the free surface to be  $z(t) = x(t) + iy(t)$ . The vertical wall is parametrised by  $\tau$ , and the point  $\xi$  on the wall is given by  $0 + iy(\tau) = iy_c\tau$ .

In terms of the arclength parameter the kinematic condition (4) becomes

$$\psi'(t) = 0 \quad (8)$$

and Bernoulli's equation (3) is

$$\frac{1}{2}\phi'(t)^2 + y(t) = \frac{1}{2}F^2 + 1. \quad (9)$$

In addition, the arclength condition must also be satisfied, and this is

$$x'(t)^2 + y'(t)^2 = 1. \quad (10)$$

Taking the imaginary part of Equation (7) yields the following two forms of the integral equation, depending on whether the point  $z$  lies on the free surface or the vertical wall. For  $z$  on the free surface, we denote its position by  $z(s)$  and after applying the kinematic condition

(8) the integral equation becomes

$$\begin{aligned}
 & -\pi[\phi'(s)x'(s) - \mu(s)] + \int_0^\infty \frac{\Phi(t)[y(t) - y(s)] - \Psi(t)[x(t) - x(s)]}{[x(t) - x(s)]^2 + [y(t) - y(s)]^2} dt \\
 & + \int_0^\infty \frac{\Phi(t)[y(t) + y(s)] - \Psi(t)[x(t) - x(s)]}{[x(t) - x(s)]^2 + [y(t) + y(s)]^2} dt \\
 & + \int_0^1 \frac{y_c \Upsilon(\tau)[y_c \tau - y(s)]}{x(s)^2 + [y_c \tau - y(s)]^2} d\tau + \int_0^1 \frac{y_c \Upsilon(\tau)[y_c \tau + y(s)]}{x(s)^2 + [y_c \tau + y(s)]^2} d\tau = 0.
 \end{aligned} \tag{11}$$

For convenience of display we have defined the intermediate variables

$$\begin{aligned}
 \Phi(t) &= [\phi'(t) - \mu(t)x'(t) - \nu(t)y'(t)], \\
 \Psi(t) &= [\nu(t)x'(t) - \mu(t)y'(t)], \\
 \Upsilon(\tau) &= [\nu(\tau) - \nu(\tau)].
 \end{aligned} \tag{12}$$

For  $z$  on the wall, we denote its position by  $iy_c\sigma$ , and then the integral equation reduces to

$$\begin{aligned}
 & \int_0^\infty \frac{\Phi(t)[y(t) - y_c\sigma] - \Psi(t)x(t)}{x(t)^2 + [y(t) - y_c\sigma]^2} dt + \int_0^\infty \frac{\Phi(t)[y(t) + y_c\sigma] - \Psi(t)x(t)}{x(t)^2 + [y(t) + y_c\sigma]^2} dt \\
 & + \int_0^1 \frac{\Upsilon(\tau)}{[\tau - \sigma]} d\tau + \int_0^1 \frac{\Upsilon(\tau)}{[\tau + \sigma]} d\tau = 0.
 \end{aligned} \tag{13}$$

Our task is now to find the functions  $y(t)$ ,  $x(t)$ ,  $y'(t)$ ,  $x'(t)$ ,  $\phi'(t)$ ,  $\Upsilon(\tau)$  that satisfy Equations (9–13).

### 3. Numerical method

In this section we use a numerical procedure similar to that employed by Forbes [20]. First, however, we introduce the transformation

$$t = e^\rho - 1. \tag{14}$$

Discretisation of the flow variables on the free surface onto a mesh of  $N$  evenly spaced  $\rho$  points results in a clustering of points in the arclength variable  $t$ , about the cusp point  $(x(0), y(0)) = (0, y_c)$ . The vertical wall is divided up onto a mesh of  $M$  evenly spaced  $\tau$  points. The notation  $y_i$ , for example, shall be used to represent the value of the function  $y$  evaluated at the  $i$ th meshpoint  $\rho_i$ . Similarly  $\Upsilon_j = \Upsilon(\tau_j)$ . These two different meshes coincide at the cusp point  $\rho_1 = 0, \tau_M = 1$ .

The vector of  $N + M - 3$  unknowns is

$$[y'_2, \dots, y'_N, \Upsilon_2, \dots, \Upsilon_{M-1}],$$

since  $y'_1 = 1$  and  $\Upsilon_1 = 0$  are known in advance and  $\Upsilon_M$  can be calculated. Given an initial guess at the vector of unknowns, we can evaluate  $x'_i$  from the arclength condition (10). Then, we use trapezoidal integration to calculate  $y_i$  integrating back from the far-stream height of

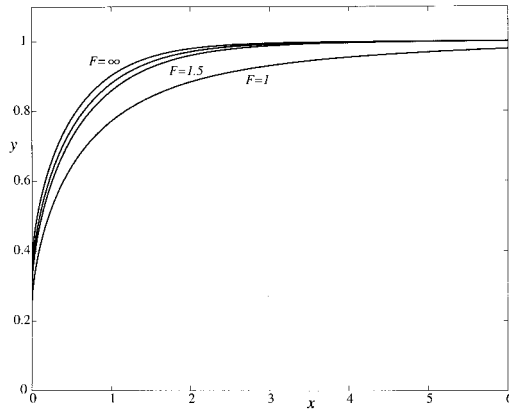


Figure 2. Three free surface profiles for the limiting case  $L \rightarrow 0$ . The Froude numbers are  $F = 1$ ,  $F = 1.5$ ,  $F = 2$  and  $F = \infty$ .

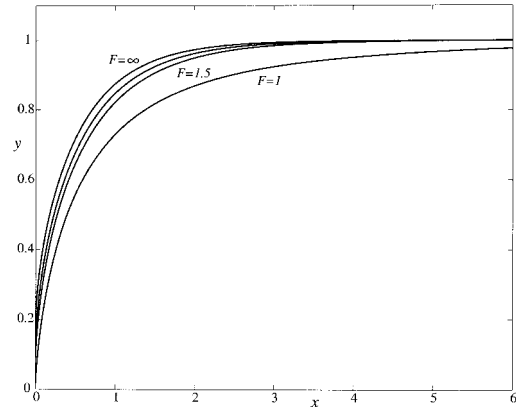


Figure 3. Three free surface profiles for a sink width of  $L = 0.5$  and Froude numbers are  $F = 1$ ,  $F = 1.5$ ,  $F = 2$  and  $F = \infty$ .

$y = 1$  and  $x_i$  integrating forward from  $x = 0$ . The values obtained for  $y_i$  are then used in Bernoulli's equation (9) to calculate the values of  $\phi'_i$ . Lastly  $\Upsilon_M = \phi'_1 y'_1 - v_M$ .

The integral equation (11) is evaluated at the  $N - 1$  half-mesh points  $\{\rho_{i+1/2}, i = 1 \dots N - 1\}$ , and the integral equation (13) is evaluated at the  $M - 2$  half-mesh points  $\{\sigma_{j+1/2}, j = 2 \dots M - 1\}$ . Values for the flow variables at these half-mesh points are determined by linear interpolation from the values at the whole-mesh points. The singularities in the Cauchy principal value integrals can now be ignored since they occur symmetrically between mesh points. Trapezoidal rule integration is used for both integrals.

This gives us a system of  $N + M - 3$  equations for the  $N + M - 3$  unknowns and this system is solved by a damped Newton's method.

Typically 600 points are used on the free surface, truncating at  $\rho = 2.5$ , giving  $\Delta\rho = 0.0041667$ . In terms of arclength, this corresponds to truncating at  $t \approx 11.2$ , with a minimum  $\Delta t \approx \Delta\rho$  and a maximum  $\Delta t \approx 0.051$  at the truncation point. In the case of solutions for  $F = 1$  the same  $\Delta\rho$  is used but the truncation point is extended out to  $\rho = 3$ ,  $t \approx 19.1$ , due to the slow convergence of such solutions in the far field to the undisturbed fluid depth (see Figures 2 and 3). On the wall 80 points were typically used, giving a mesh spacing  $\Delta\tau = 0.0125$  there. The value of  $\Delta y = y_c \Delta\tau$  on the wall varies as  $y_c$  varies. But, since  $y_c < 0.37$  (see Section 4)  $\Delta y < 0.0046$ .

Decreasing these step sizes was not found to affect the solutions significantly and comparisons with limiting solutions computed elsewhere were found to be in good agreement (see Section 4), indicating well converged solutions.

#### 4. Discussion of results

In the limit that  $L \rightarrow 0$ , the extended sink reduces to the familiar line sink and we shall consider flow in this regime first. As has been found previously (Hocking [12], Vanden-Broeck and Keller [13]), cusp solutions for flow into a line sink exist only for Froude numbers  $F \geq 1$ , except for a unique branch of cusp solutions for sinks off the bottom occurring at Froude

Table 1. A table of the cusp heights  $y_c$  versus Froude numbers  $F$  for the four cases that the sink width  $L = 0$ ,  $L = 0.2$ ,  $L = 0.5$ , and  $L = 0.7$ . The last entry (marked  $\infty^*$ ) denotes the exact solution of King and Bloor [15].

$F$	$L = 0$	$L = 0.2$	$L = 0.5$	$L = 0.7$
1.0	0.247	0.201	0.017	—
1.2	0.275	0.234	0.047	—
1.5	0.302	0.266	0.090	0.004
2.0	0.327	0.294	0.133	0.020
3.0	0.347	0.317	0.169	0.047
5.0	0.358	0.330	0.190	0.067
$\infty$	0.364	0.337	0.201	0.081
$\infty^*$	0.363			

numbers less than one (Vanden-Broeck and Keller [13]). Since our sink always lies on the bottom, this branch of solutions is not recovered.

An exact analytic solution exists in the limit as the Froude number tends to infinity, as found by King and Bloor [15]. We compute a solution for  $F \rightarrow \infty$  by analytically determining the limiting forms of Equations (9, 11, 13) and then solving them, using the numerical method outlined above. A comparison between our solution and the exact solution shows that they are almost identical, and indeed show no graphical difference on the scale of the far-stream height, unity. Our solutions unfortunately exhibit their greatest error right at the cusp point, but a comparison between the computed cusp height  $y_c \approx 0.364$  with the exact cusp height  $y_c^* = 1 - 2/\pi \approx 0.36338$  still shows very good agreement.

Provided that the truncation point  $\rho_N$  is suitably large, so that  $y_N \approx 1$  ( $\rho_N \approx 1.8$  for  $F = \infty$ , giving  $x_N \approx 5$ ),  $y_c$  is independent of the actual value of  $\rho_N$ , instead varying only with the mesh sizes  $\Delta\rho$ . Halving the mesh size on the free surface and the vertical wall results in a slightly improved estimate for the cusp height, but it still rounds to 0.364. However due to the matrix system that must be solved repeatedly in the numerical method, halving the mesh size is much more computationally intensive.

In Figure 2 we graph three free surface profiles for  $L = 0$ . Shown are the profiles obtained for the limiting Froude numbers  $F = 1$  and  $F = \infty$  and for the intermediate values  $F = 1.5$ , and  $F = 2$ . A list of cusp heights versus Froude number is given in Table 1.

We now turn our attention back to the problem of the extended sink, where  $L \neq 0$ . As for the  $L = 0$  case, solutions are only found to exist for supercritical flow,  $F \geq 1$ . Three free-surface profiles are shown in Figure 3 for  $L = 0.5$  and  $F = 1$ ,  $F = 1.5$ ,  $F = 2$  and  $F = \infty$ . In all three cases, the cusp height, where the free surface attaches smoothly to the wall, can seem to be much lower than the  $L = 0$  case in Figure 2. This can also be seen in an examination of Table 1, which lists cusp height versus Froude number for  $L = 0$  and  $L = 0.5$ , as well as  $L = 0.2$  and  $L = 0.7$ . Furthermore, most of the variation in these profiles can be seen to occur between  $F = 1$  and  $F = 2$  for both the  $L = 0$  and  $L = 0.5$  cases. This fact has been observed previously by Wen and Ingham [21] and Hocking [18].

For a given Froude number, as we increase the sink width  $L$  the cusp height  $y_c$  decreases until it finally drops to touch the sink at  $y = 0$  where  $L = L^{\text{crit}}$ . This is, however, exactly the

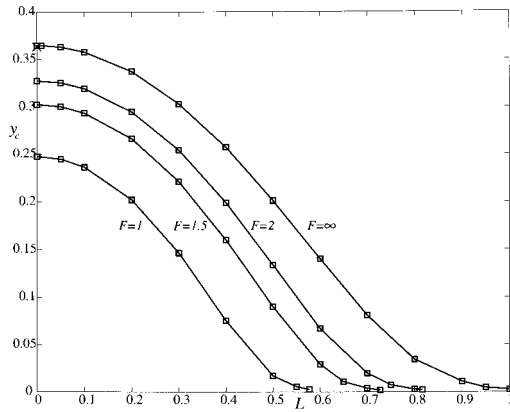


Figure 4. A plot of cusp height  $y_c$  vs sink width  $L$  for the Froude numbers  $F = 1$ ,  $F = 1.5$ ,  $F = 2$ , and  $F = \infty$ . The markers indicate the actual computed values. The cross at  $(0, 0.3634)$  represents the value for the exact solution.

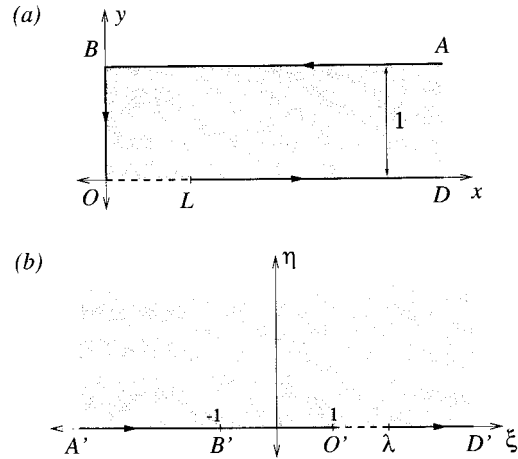


Figure 5. (a) A sketch of the physical  $z$ -plane and (b) the  $z$ -plane mapped to the upper half  $\zeta$  plane.

limiting configuration found in Koerber and Forbes [22], for which the critical sink width for vertical entry is given by

$$L^{\text{crit}}(F) = \frac{F}{\sqrt{F^2 + 2}}. \tag{15}$$

For  $F = 1$ ,  $L^{\text{crit}}(1) \approx 0.57735$  and in the limit as  $F \rightarrow \infty$ ,  $L^{\text{crit}}(\infty) = 1$ .

In Figure 4, four plots of  $y_c$  versus  $L$  are shown, for  $F = 1$ ,  $F = 1.5$ ,  $F = 2$ , and  $F = \infty$ . The computed cusp height at  $L = L^{\text{crit}}$  doesn't quite reach zero in any of these plots. This is not surprising since the formulation explicitly builds in the presence of the vertical wall. A comparison between the solutions presented here, and those calculated in Koerber and Forbes [22] for the limiting cases that  $L = L^{\text{crit}}$ , show excellent agreement.

If  $L$  is increased beyond  $L^{\text{crit}}$ , no cusp solutions are found. Instead, we expect the solutions of Koerber and Forbes [22] to be obtained in these parameter regions, in which the free surface is drawn down directly into the sink. Physically the process of increasing  $L$  involves decreasing  $V$  in proportion, as  $V = F/L$ . So if the uniform outflow profile were being created by some kind of mesh or mat over an outflow pump, then a constant outflow volume would have to be maintained.

Alternatively, let us imagine a flow into a sink of fixed width with some large Froude number and corresponding outflow velocity. As we decrease  $F$ , a minimum  $F_{\text{min}}$  will be reached at which the cusp height has decreased to zero and after which no solutions of this type can be found, as described above. From Equation (15) we have  $F_{\text{min}} = 1$  up until  $L = L^{\text{crit}}(1) \approx 0.577$  and then  $F_{\text{min}} \rightarrow \infty$  as  $L \rightarrow 1$ . This is very similar to the behaviour shown in Hocking [18] for flow into (from) a vertical slot, where a plot of the minimum Froude number for which solutions exist against the slot width shows  $F_{\text{min}} = 1$  up to a slot width of about 0.5 and then  $F_{\text{min}} \rightarrow \infty$  as the slot width tends to one.



## 5. Summary and conclusions

Solutions have been obtained for all extended sink widths  $L \leq 1$ , unity being the case when the sink width is the same as the far-stream depth. For  $L \leq 0.577$  solutions exist for all values of the Froude number  $F \geq 1$ . For sink widths greater than this critical value, solutions only exist down to a minimum Froude number greater than one, this minimum tending to infinity as  $L$  approaches unity. This behaviour is very similar to that found by Hocking [18] for flow into a vertical slot. No subcritical solutions were found.

For sink widths greater than unity, steady solutions of the type obtained by Koerber and Forbes [22] are expected to occur. In these solutions, the free surface is drawn right down into the sink. This conclusion is supported by the fact that our solutions in the present paper fail at precisely the values of the drain width (or Froude number) at which the Koerber and Forbes [22] solutions commence.

In the limit that the sink width tends to zero, the solutions for a line sink found by previous authors (Hocking [12], Vanden-Broeck and Keller [13], King and Bloor [15]) are recovered, and a table of cusp height versus Froude number is provided for reference. Furthermore, the solutions computed here have been compared directly against those of King and Bloor [15] and Koerber and Forbes [22], for the appropriate limiting configurations, and have been shown to be very accurate.

The technique employed in this paper to find solutions for a uniform outflow velocity profile across the extended sink could be used to find solutions for any vertical outflow velocity profile  $V(x)$ . Previous experience in the drawn-down case however (Koerber and Forbes [22]), indicates that such solutions would be qualitatively similar to the ones presented here.

It remains unclear what happens in the subcritical case, with Froude numbers less than one. It may be that stagnation point solutions occur, or that only time dependent solutions exist.

### Appendix: The rigid-lid solution

Here we solve for the complex potential  $g(z)$  that represents the solution for the flow into an extended sink in a corner with a rigid lid. More specifically, we derive an expression for the complex velocity

$$\frac{dg}{dz} = \mu - i\nu, \quad (\text{A1})$$

where  $\mu$  is the horizontal velocity component and  $\nu$  the vertical component for this flow.

In the physical  $z$ -plane, the flow region is bounded by the flat bottom  $y = 0$  for  $x > L$  and the extended sink in the corner for  $0 \leq x \leq L$ , by the vertical wall at  $x = 0$  for  $0 \leq y \leq 1$  and by the rigid lid  $y = 1$ . Since there is no flow through the walls, and the vertical outflow velocity for the extended sink is  $-V$ , the boundary conditions are then

$$\nu = 0 \quad \text{on} \quad y = 1, \quad (\text{A2})$$

$$\mu = 0 \quad \text{on} \quad x = 0 \quad (0 \leq y \leq 1), \quad (\text{A3})$$

$$\nu = 0 \quad \text{on} \quad y = 0, \quad x > L, \quad (\text{A4})$$

$$\nu = -V \quad \text{on} \quad y = 0, \quad 0 \leq x \leq L. \quad (\text{A5})$$

By making use of the conformal mapping

$$\zeta = \cosh(\pi z) \quad (\text{A6})$$

we map the flow region in the  $z$ -plane into the upper-half  $\zeta$ -plane, as shown in Figure 5, where  $\zeta = \xi + i\eta$  and  $\lambda = \cosh(\pi L)$ . The entire boundary in the physical plane is now mapped to the line  $\eta = 0$  in the  $\zeta$ -plane.

Flow in the  $\zeta$ -plane is then generated by a distribution of line sinks placed along the interval  $\xi \in [1, \lambda]$  as follows;

$$g(\zeta) = - \int_1^\lambda \frac{m(\sigma)}{2\pi} \log(\zeta - \sigma) d\sigma. \quad (\text{A7})$$

This distribution automatically satisfies the first three of the boundary conditions (A2–A4), since there will be no vertical component of velocity along the line  $\eta = 0$  outside of the interval  $[1, \lambda]$ . We now seek to calculate the sink strengths  $m(\sigma)$  so that the final boundary condition (A5) is satisfied.

We have

$$\frac{dg}{dz} = \frac{dg}{d\zeta} \frac{d\zeta}{dz}$$

and therefore obtain

$$\mu - i\nu = \frac{dg}{d\zeta} \pi \sqrt{\zeta^2 - 1} = \frac{1}{2} \int_1^\lambda \frac{m(\sigma) \sqrt{\zeta^2 - 1}}{\zeta - \sigma} d\sigma. \quad (\text{A8})$$

Now using the extended sink boundary condition (A5) together with Equation (A8) we have

$$-V = \lim_{\eta \rightarrow 0} \Im \left\{ \frac{1}{2} \int_1^\lambda \frac{m(\sigma) \sqrt{\zeta^2 - 1}}{\zeta - \sigma} d\sigma \right\}.$$

After evaluating the imaginary part we make use of the substitution

$$\xi - \sigma = \eta\theta$$

and then take the limit to yield the following expression for the sink strengths;

$$m(\xi) = \frac{2V}{\pi \sqrt{\xi^2 - 1}}. \quad (\text{A9})$$

Substituting (A9) back in Equation (A8) gives the following integral form for  $dg/dz$ ,

$$\frac{dg}{dz} = -\frac{V}{\pi} \int_1^\lambda \frac{\sqrt{\zeta^2 - 1}}{\sqrt{\sigma^2 - 1}} \frac{1}{\zeta - \sigma} d\sigma. \quad (\text{A10})$$

The integration in Equation (A10) can be carried out in closed form, giving

$$\frac{dg}{dz} = -\frac{2V}{\pi} \operatorname{arctanh} \left( \sqrt{\frac{\zeta + 1}{\zeta - 1}} \sqrt{\frac{\lambda - 1}{\lambda + 1}} \right). \quad (\text{A11})$$

Finally, substituting in for  $\zeta$  and  $\lambda$  from Equation (A6), we obtain the solution

$$\frac{dg}{dz} = -\frac{2V}{\pi} \operatorname{arctanh} \left( \coth \left( \frac{\pi z}{2} \right) \tanh \left( \frac{\pi L}{2} \right) \right). \quad (\text{A12})$$

We take the real and imaginary parts of the above Equation (A12) to get

$$\mu = -\frac{V}{2\pi} \log \left( \frac{(a+1)^2 + b^2}{(a-1)^2 + b^2} \right), \quad (\text{A13})$$

$$\nu = \frac{V}{\pi} \left( \arctan \left( \frac{b}{a+1} \right) + \arctan \left( \frac{b}{1-a} \right) \right), \quad (\text{A14})$$

where

$$a = \frac{c \sinh(\pi x)}{\cosh(\pi x) - \cos(\pi y)},$$

$$b = \frac{-c \sin(\pi y)}{\cosh(\pi x) - \cos(\pi y)},$$

$$c = \tanh \left( \frac{\pi L}{2} \right).$$

### Acknowledgements

The work of A. J. Koerber has been supported by an Australian Postgraduate Award and a Departmental Scholarship from the Department of Mathematics, University of Queensland. A. J. Koerber would like to thank S. W. McCue for many useful discussions on the inclusion of the ‘wall’.

### References

1. J. Imberger and P. F. Hamblin, Dynamics of lakes, reservoirs, and cooling ponds. *Ann. Rev. Fluid Mech.* 14 (1982) 153–187.
2. H. Mekias and J.-M. Vanden-Broeck, Subcritical flow with a stagnation point due to a source beneath a free surface. *Phys. Fluids A* 3 (1991) 2652–2658.
3. E. O. Tuck and J.-M. Vanden-Broeck, A cusp-like free-surface flow due to a submerged source or sink. *J. Austral. Math. Soc. Ser. B* 25 (1984) 443–450.
4. J. Imberger, Selective withdrawal: a review. In: *2nd International Symposium on Stratified Flows*, Trondheim, Norway (1980).
5. P. A. Tyvand, Unsteady free-surface flow due to a line source. *Phys. Fluids A* 4 (1992) 671–676.
6. L. K. Forbes and G. C. Hocking, Flow caused by a point sink in a fluid having a free surface. *J. Austral. Math. Soc. Ser. B* 32 (1990) 231–249.
7. L. K. Forbes, G. C. Hocking and G. A. Chandler, A note on withdrawal through a point sink in a fluid of finite depth. *J. Austral. Math. Soc. Ser. B* 37 (1996) 406–416.
8. Q.-N. Zhou and W. P. Graebel, Axisymmetric draining of a cylindrical tank with a free surface. *J. Fluid Mech.* 221 (1990) 511–532.
9. T. Miloh and P. A. Tyvand, Nonlinear transient free-surface flow and dip formation due to a point sink. *Phys. Fluids A* 5 (1993) 1368–1375.

10. M. Xue and D. K. P. Yue, Nonlinear free-surface flow due to an impulsively started submerged point sink. *J. Fluid Mech.* 364 (1998) 325–347.
11. L. K. Forbes and G. C. Hocking, The bath-plug vortex. *J. Fluid Mech.* 284 (1995) 43–62.
12. G. C. Hocking, Cusp-like free-surface flows due to a submerged source or sink in the presence of a flat or sloping bottom. *J. Austral. Math. Soc. Ser. B* 26 (1985) 470–486.
13. J.-M. Vanden-Broeck and J. B. Keller, Free surface flow due to a sink. *J. Fluid Mech.* 175 (1987) 109–117.
14. G. C. Hocking, Infinite Froude number solutions to the problem of a submerged source or sink. *J. Austral. Math. Soc. Ser. B* 29 (1988) 401–409.
15. A. C. King and M. I. G. Bloor, A note on the free surface induced by a submerged source at infinite Froude number. *J. Austral. Math. Soc. Ser. B* 30 (1988) 147–156.
16. G. C. Hocking, Critical withdrawal from a two-layer fluid through a line sink. *J. Eng. Math.* 25 (1991) 1–11.
17. G. C. Hocking, Supercritical withdrawal from a two-layer fluid through a line sink. *J. Fluid. Mech.* 297 (1995) 37–47.
18. G. C. Hocking, Flow from a vertical slot into a layer of finite depth. *Appl. Math. Mod.* 16 (1992) 300–306.
19. G. C. Hocking and J.-M. Vanden-Broeck, Draining of a fluid of finite depth into a vertical slot. *Appl. Math. Mod.* 21 (1997) 643–649.
20. L. K. Forbes, On the effects of non-linearity in the free surface flow about a submerged point vortex. *J. Eng. Math.* 19 (1985) 139–155.
21. X. Wen and D. B. Ingham, Flow induced by a submerged source or sink in a three layer fluid. *Computers and Fluids* 21 (1992) 133–144.
22. A. J. Koerber and L. K. Forbes, Two-dimensional steady free surface flow into a semi-infinite mat sink. *Phys. Fluids* 10 (1998) 2781–2785.